

Electronic Supplementary Information for:

Investigating isomer specific photoprotection in a model plant sunscreen

M. D. Horbury,^a A. L. Flourat,^b S. E. Greenough,^a F. Allais,^b and V. G. Stavros^{a}*

a. Department of Chemistry, University of Warwick, Gibbet Hill, Coventry, CV4 7AL

b. Chaire ABI-AgroParisTech, CEBB, 3 rue des Rouges Terres, 51110 Pomacle, France

Transient Electronic Absorption Spectroscopy Method

The femtosecond transient electronic absorption spectroscopy (TEAS) setup used to monitor the dynamical processes has been described in detail previously,^{1,2} however, details specific to the present experiments are provided herein. The probe pulse was a broadband white light continuum generated in a CaF₂ window with a thickness of 1 mm, providing a probe window of 330 – 675 nm.

The fs pump pulses were produced using an optical parametric amplifier, (TOPAS-C, Spectra-Physics), with a fluence of 200 – 800 $\mu\text{J}\cdot\text{cm}^{-2}$. The pump excitation wavelengths were 319 nm for *Z*- and *E*-ethyl sinapate in cyclohexane.

The pump-probe time delay (Δt) was varied by adjusting the optical delay of the probe pulse, the maximum obtainable Δt was 2 nanoseconds (ns). Changes in the optical density (ΔOD) of the samples were calculated from probe intensities, collected using a spectrometer (Avantes, AvaSpec-ULS1650F).

The solutions of ethyl sinapate were made to a concentration of 1 mM in cyclohexane (99.99%, VWR). The delivery system for the samples was a flow-through cell (Demountable Liquid Cell by Harrick Scientific Products Inc.) consisting of two CaF₂ windows with a thickness of 1 mm for the front window and 2 mm for the back window. The windows were spaced a 100 μm apart to limit temporal dispersion of the pump and probe pulses. The sample was circulated using a diaphragm pump (SIMDOS, KNF) recirculating sample from a 50 mL reservoir in order to provide each pulse with fresh sample.

Steady State Difference Spectra

Steady-state difference absorption spectra, ' $\Delta\text{UV}/\text{vis}$ spectra' were collected to determine the spectral signature of the isomer-photoproduct of ethyl sinapate. The $\Delta\text{UV}/\text{vis}$ spectrum for ethyl sinapate in cyclohexane was acquired by irradiating the solution using an arc lamp (Fluorolog 3, Horiba) for 10 min at the corresponding TEAS excitation wavelength using an 8 nm bandwidth. The 'before' and 'after' UV-vis spectra were measured using a UV-vis spectrometer (Lambda 850, PerkinElmer). The difference spectrum was generated by subtracting the 'before' spectrum from the 'after' spectrum.

Synthesis of *Z*- and *E*-ethyl sinapate

Materials

All reagents were provided by Sigma Aldrich, solvents were provided by Fisher-Scientific (THF) and VWR (AcOEt and cyclohexane). Deuterated chloroform was provided by Euriso-Top. Evaporations were conducted on Rotavap R-300, Büchi, equipped with a PC3001 Vario^{pro} pump, Vacuubrand. Purifications were conducted using Puriflash 4100, Interchim with pre-packed silica gel column (30 μ m, Interchim PF-Si30-HP). NMR spectra were recorded on a Fourier 300, Bruker; ¹H spectra and ¹³C spectra were calibrated on CDCl₃ residual peak, δ = 7.26 and 77.16 ppm respectively.

O-Acetylated *Z*-Ethyl sinapate

5.0 g of syringaldehyde (27 mmol) was dissolved in Pyridine (34 mL) and acetic anhydride was added (30 mL). The reaction was stirred overnight at room temperature and poured into acidified iced water (150 mL). The mixture was extracted thrice with ethyl acetate. Organic phases were combined, washed with brine, dried over anhydrous magnesium sulfate, filtered and concentrated. *O*-Acetylated syringaldehyde was recovered (quantitative yield) and used for the next step without further purification.

Under nitrogen, ethyl [bis(2,2,2-trifluoroethoxy)phosphinyl]acetate (634 μ L, 2.7 mmol) and 18-crown-6 (707 mg, 2.7 mmol) were dissolved in dry THF (15 mL). At -78 °C, a solution of potassium bis(trimethylsilyl)amide, KHMDS, (535 mg, 2.7 mmol) in dry THF (10 mL) was added dropwise to the previous solution for *ca.* 20 min. The reaction mixture was stirred for a further 30 min, before the dropwise addition of a solution of *O*-acetylated syringaldehyde (500 mg, 2.2 mmol) in dry THF (10 mL) for 20 min. The reaction mixture was then brought to room temperature and stirred for 4 hours and subsequently quenched with a saturated solution of ammonium chloride and extracted with ethyl acetate. The organic layers were combined and washed with brine, dried over anhydrous magnesium sulfate, then filtered and concentrated. Flash chromatography (0 to 15% of AcOEt in cyclohexane) was performed. Fractions containing the desired product were combined and concentrated. 521 mg of desired product (80%) was recovered.

Deprotection of *O*-Acetylated *Z*-Ethyl sinapate

With piperazine:

500 mg of *O*-acetylated *Z*-Ethyl sinapate (1.7 mmol) was dissolved in THF (20 mL) and piperazine was added (576 mg, 6.7 mmol). The reaction was stirred for 2 hours at room temperature. THF was removed by evaporation. The crude product was diluted into AcOEt and washed twice with HCl (1M) and then brine, dried over anhydrous magnesium sulfate, filtered and concentrated. Flash chromatography was performed (10 to 15% of AcOEt in cyclohexane) and *E*-isomer was recovered (98%).

With Hydrochloric acid:

250 mg of *O*-acetylated *Z*-Ethyl sinapate (0.85 mmol) was dissolved in acetone (57 mL) and a 3 M solution of hydrochloric acid (17 mL) was added. The reaction was refluxed overnight, then cooled to

room temperature. 200 mL of AcOEt was added and the mixture was washed with water and then brine, dried over anhydrous magnesium sulphate, filtered and concentrated. NMR of the crude product revealed a trace of starting materials and *E*-isomer.

Z-ethyl sinapate

Under nitrogen, ethyl [bis(2,2,2-trifluoroethoxy)phosphinyl]acetate (520 μ L, 2.2 mmol) and 18-crown-6 (582 mg, 2.2 mmol) were dissolved in dry THF (15 mL). At -78 $^{\circ}$ C, a solution of potassium bis(trimethylsilyl)amide, KHMDS, (439 mg, 2.2 mmol) in dry THF (9 mL) was added dropwise to the previous solution for *ca.* 20 min. The reaction mixture was stirred for a further 30 min, before the dropwise addition of a solution of syringaldehyde (365 mg, 2.0 mmol) in dry THF (9 mL) for 20 min. The reaction mixture was then brought to room temperature and stirred for 4 hours and subsequently quenched with a saturated solution of ammonium chloride and extracted with ethyl acetate. The organic layers were combined and washed with brine, dried over anhydrous magnesium sulfate, then filtered and concentrated. Flash chromatography (10% to 15% of AcOEt in cyclohexane) was performed to eliminate any unreacted syringaldehyde and *E*-ethyl sinapate. Fractions containing the desired product were combined, concentrated, diluted in pure cyclohexane then centrifugated at 14.5 G, 15 $^{\circ}$ C for 10 min to remove phosphonate residue. The upper phase containing the desired product was repurified by flash chromatography. 30 mg (6% yield) of the *Z*-ES product with very high purity was recovered.

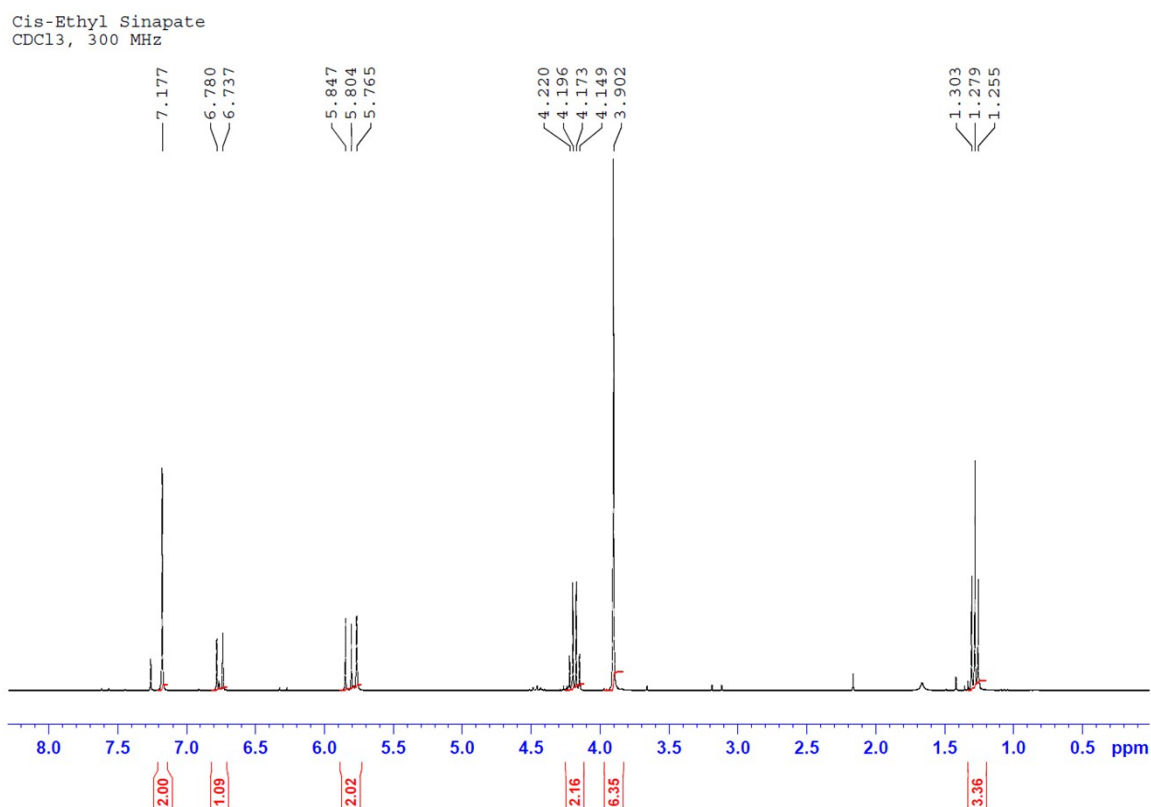


Figure S1: NMR ^1H δH (300 MHz, CDCl_3) 1.28 (t, 3H, $J=7.2$ Hz, $\text{H}_{\text{CH}_2\text{CH}_3}$), 3.90 (s, 6H, H_{OMe}), 4.18 (quad, 2H, $J=7.2$ Hz, $\text{H}_{\text{CH}_2\text{CH}_3}$), 5.77 (s, 1H, H_{OH}), 5.82 (d, 1H, $J=12.9$ Hz, H_{a}), 6.76 (d, 1H, $J=12.9$ Hz, H_{b}), 7.18 (s, 2H, H_{arom}) ppm.

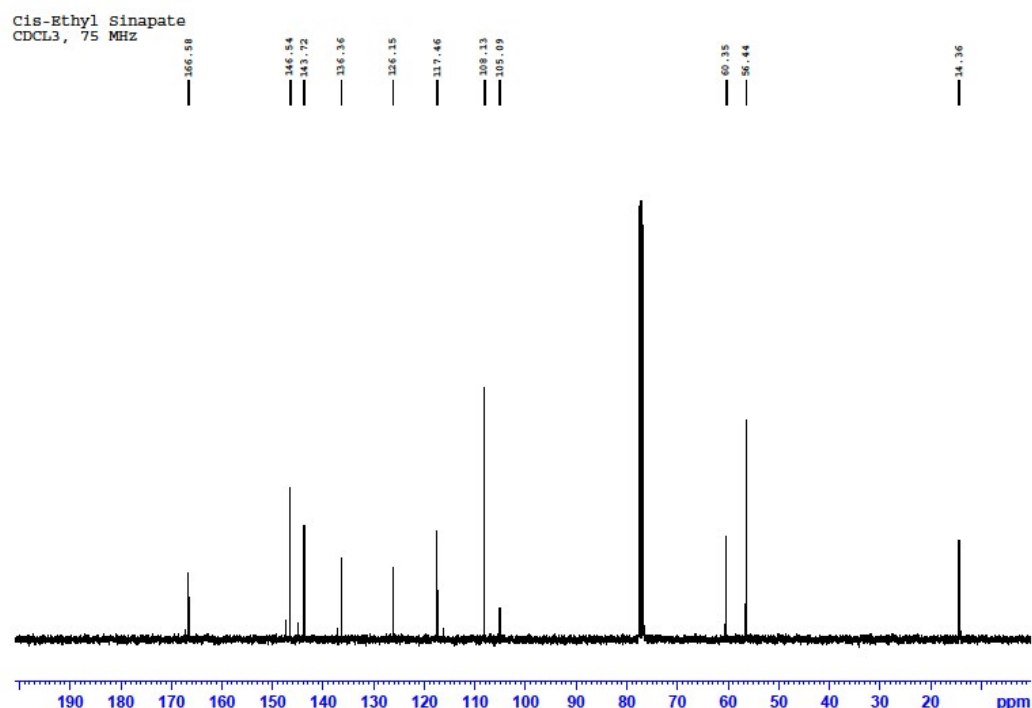


Figure S2: NMR ^{13}C δC (75 MHz, CDCl₃) 14.4 (C_{CH₂CH₃}), 56.4 (C_{OMe}), 60.4 (C_{CH₂CH₃}), 108.1 (C _{β}), 117.5 (C_{AROM}), 126.2 (C_{C=CH}), 136.4 (C_{C-OH}), 143.7 (C _{α}), 146.5 (C_{C-OMe}), 166.6 (C_{C=O}) ppm;

***E*-ethyl sinapate**

Syringaldehyde (100 g, 550 mmol), malonic acid (86 g, 825 mmol, 1.5 equiv) and aniline (5.0 ml, 55 mmol, 0.1 equiv) were mixed in pyridine (140 ml) in the dark at 60°C. The reaction mixture was poured into 500 ml of iced water and acidified with concentrated HCl until pH 2. The precipitate was filtered, washed with water until it reached neutral pH and dried. 105 g of a yellow powder of sinapic acid (85%) was recovered.

This sinapic acid (25g, 111 mmol) was dissolved in 250 ml of absolute ethanol. A few drops of concentrated HCl were added. The mixture was refluxed overnight. The crude mixture was concentrated, diluted in AcOEt, washed twice with a saturated solution of NaHCO₃, then with brine, dried over anhydrous MgSO₄, filtered and concentrated. A slightly rose powder was obtained (100%). Further purification by flash chromatography (15% of AcOEt in cyclohexane) was conducted on 1 g to obtain high purity *E*-ethyl sinapate. 0.83 g of the desired product was recovered (83%).

Trans-Ethyl Sinapate
CDCl₃, 300 MHz

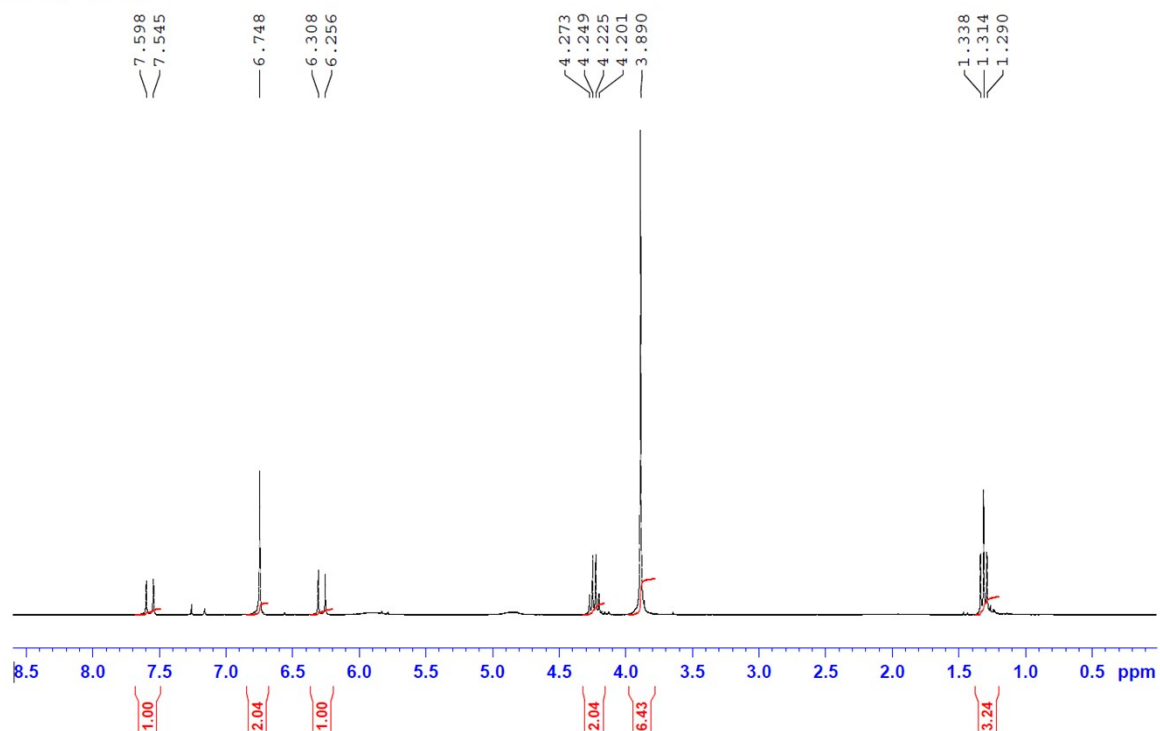


Figure S3: NMR ¹H δH (300 MHz, CDCl₃) 1.31 (t, 3H, *J*=7.2 Hz, H_{CH₂CH₃}), 3.89 (s, 6H, H_{OMe}), 4.24 (quad, 2H, *J*=7.2 Hz, H_{CH₂CH₃}), 6.28 (d, 1H, *J*=15.9 Hz, H_α), 6.75 (s, 2H, H_{arom}), 7.57 (d, 1H, *J*=15.9 Hz, H_β) ppm.

Trans-Ethyl Sinapate
CDCl₃, 75 MHz

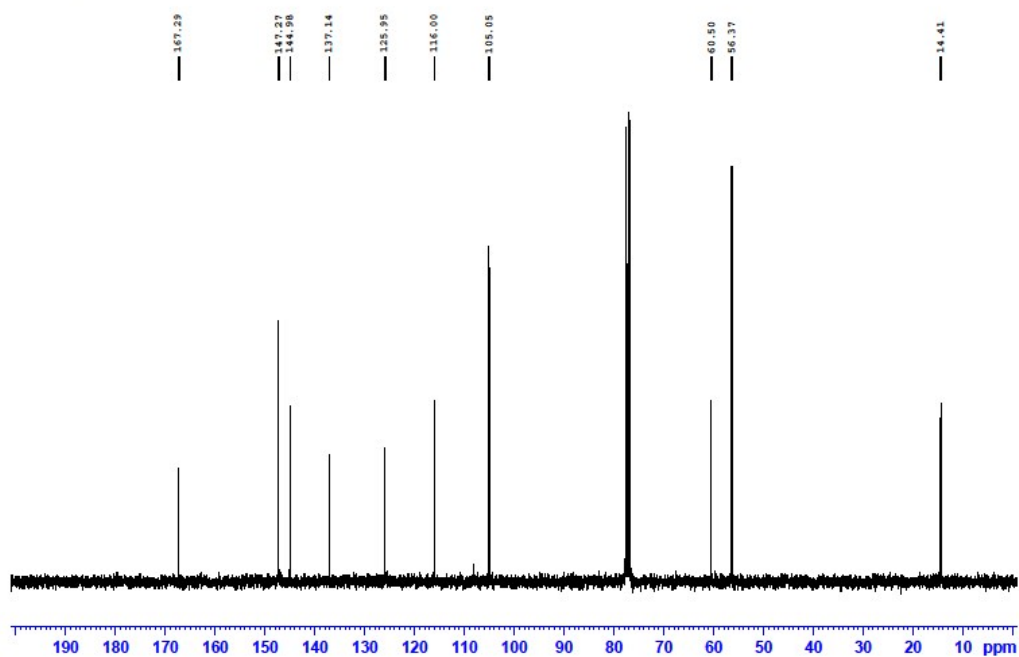


Figure S4: NMR ¹³C δC (75 MHz, DMSO-*d*₆) 14.4 (C_{CH₂CH₃}), 56.4 (C_{OMe}), 60.5 (C_{CH₂CH₃}), 105.1 (C_{arom}), 116.0 (C_β), 126.0 (C_{C-CH=CH}), 137.1 (C_{C-OH}), 145.0 (C_α), 147.3 (C_{C-OMe}), 167.3 (C_{C=O}) ppm.

305 nm Excitation of *E*-ethyl sinapate

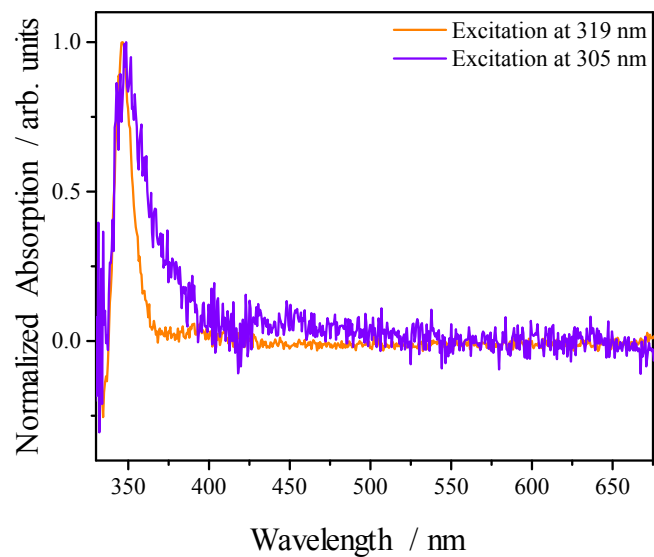


Figure S5: TAS taken at a Δt of 2 ns of *E*-ethyl sinapate in cyclohexane, excited at 319 nm (orange line) and 305 nm (purple line). The apparent broadening of the absorption feature at 305 nm is very likely indicative of an overlapping feature of the phenoxyl radical absorption.

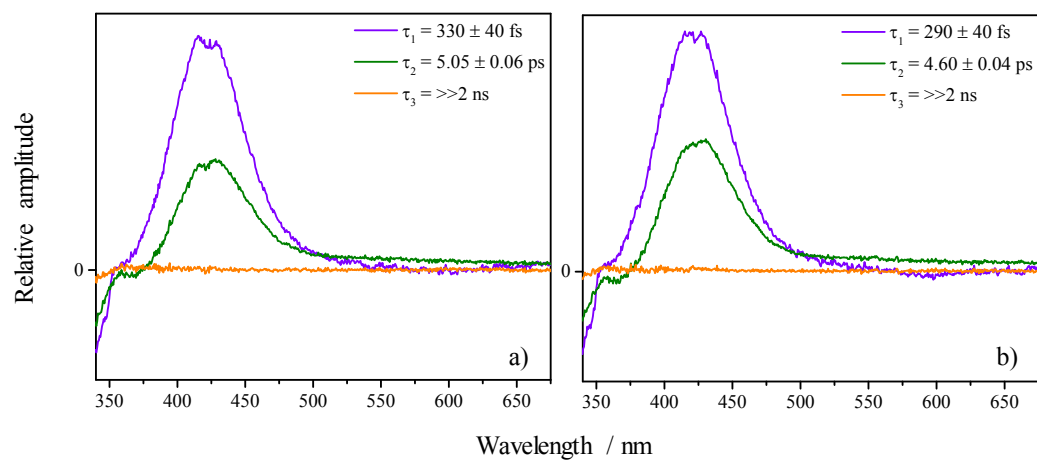


Figure S6: Resulting evolution associated difference spectra (EADS) from the sequential global fit of ethyl sinapate, a) *Z*-ethyl sinapate and b) *E*-ethyl sinapate in cyclohexane.

Sequential Global Fitting Analysis

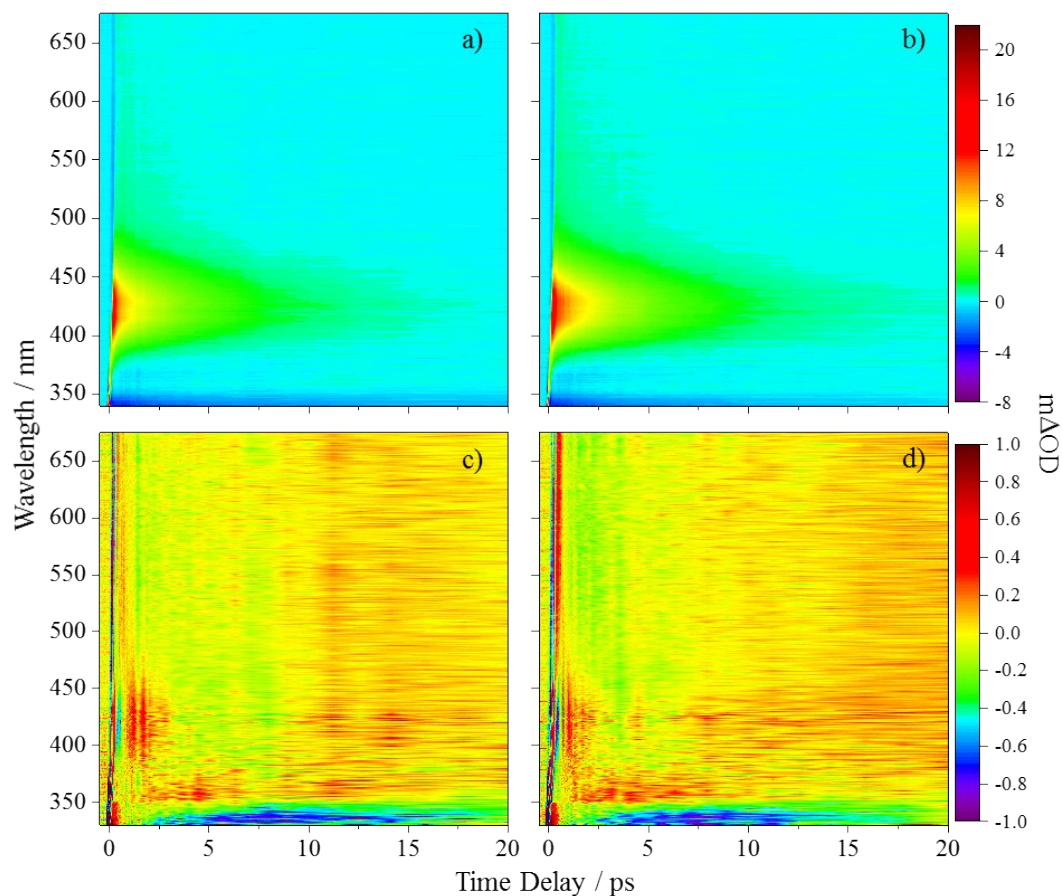


Figure S7: Full wavelength range TAS of (Z/E)-ethyl sinapate shown as false colourmaps representing the change in optical density (ΔOD) in cyclohexane a) Z-ethyl sinapate and b) E-ethyl sinapate photoexcited at 319 nm. TAS residual plot with a maximum deviation of $\sim 10\%$ for c) Z-ethyl sinapate and d) E-ethyl sinapate. We note that in the heatmaps the Z-isomer appears to decay faster than the E-isomer. This is due to them being plotted on the same intensity scale and the Z-isomer having a weaker signal strength.

Photoisomerization yield

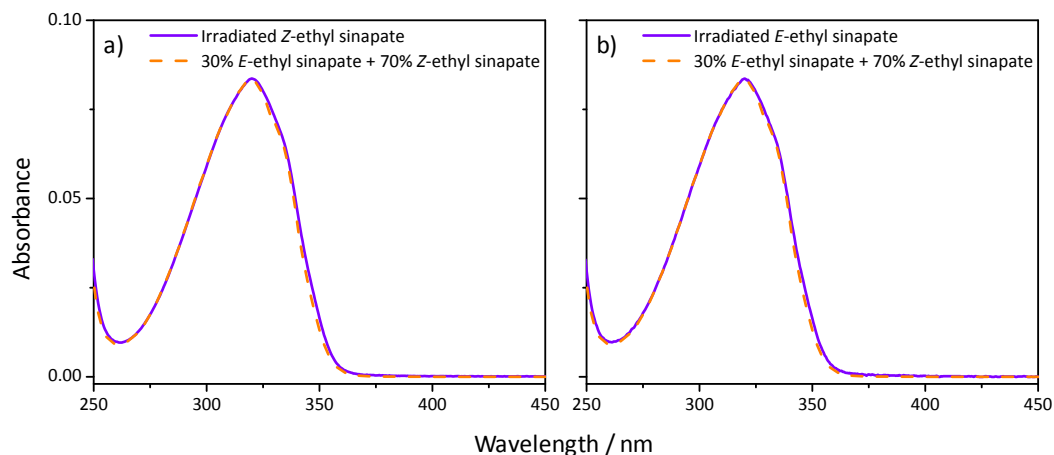


Figure S8: (a) UV/vis absorption spectrum taken following irradiation at 319 nm of pure Z-ethyl sinapate in cyclohexane for 45 mins (purple line). Overlaid is a simulated UV/vis spectrum generated *via* a linear combination of the isomer specific UV/vis spectra (see Fig. 2, main manuscript). (b) Similarly, irradiation of pure E-ethyl sinapate. The extracted ratio of isomers, following irradiation, is $70 \pm 3\%$ Z-ethyl sinapate and $30 \pm 3\%$ E-ethyl sinapate (irrespective of starting isomer). The UV irradiation source (from an arc lamp, Fluorolog 3) was centred at 319 nm with an 8 nm bandwidth and an average power of $\sim 3\text{mW}$. To ensure equilibrium was established, the samples were irradiated for 45 mins; no further changes to the absorption spectra (purple traces) were evident beyond this time.

Transient electronic absorption spectroscopy on *Z*- and *E*-ethyl sinapate in ethanol

Additional transient electronic absorption measurements were taken for *Z*- and *E*-ethyl sinapate in ethanol, to observe the effects of a polar environment on their photochemistry. The two isomers show similar spectral features and shall be discussed together. The transient absorption spectra (TAS, Figure S9) after initial excitation are dominated by a large excited state absorption (ESA) centred at 415 nm (not easily discernible on scale provided) and a ground state bleach (GSB) at ~340 nm. However, as the pump-probe time delay (Δt) increases, the initial ESA begins to decay away and two new spectral features grow in. The first of these is the appearance of a shoulder absorption forming at ~370 nm for both *Z*- and *E*-ethyl sinapate. Concomitantly to this, a negative feature begins to appear at ~460 nm (in both isomers), which corresponds to the spectral region in which other hydroxycinnamates have been shown to fluoresce.³ thus we assign this to a stimulated emission (SE). As Δt further increases the ESA and SE return to the baseline. Once the ESA and SE have decayed away completely a broad absorption is revealed, along with a GSB. The broad absorption is due to the formation of the phenoxyl radical rather than the corresponding ethyl sinapate isomer photoproduct. This due to the propensity for sinapates to undergo a step-wise two-photon ionization, which results in the formation of the phenoxyl radical.⁴⁻⁶ Due the absorption of the radical appearing in the same spectral region as any

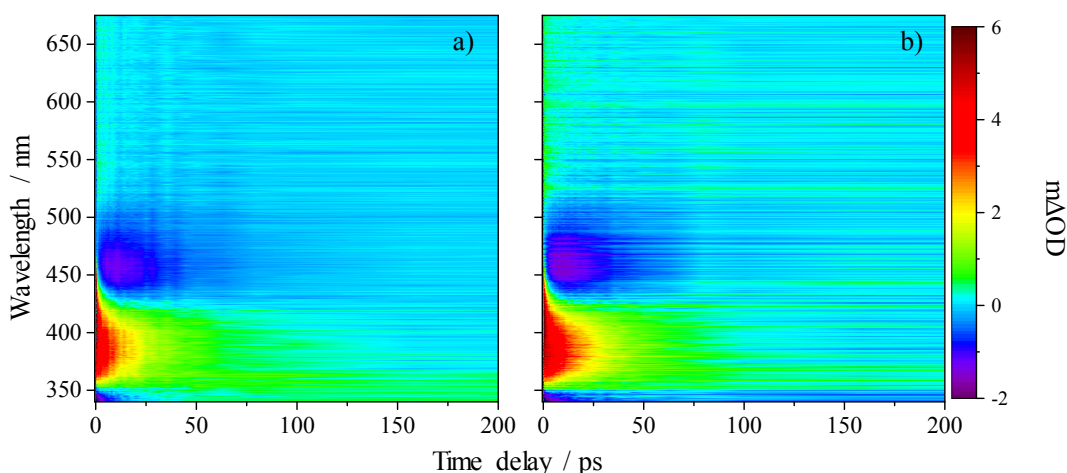


Figure S9: TAS of (*Z/E*)-ethyl sinapate shown as false colourmaps representing the change in optical density (ΔOD) in ethanol a) *Z*-ethyl sinapate photoexcited at 327 nm and b) *E*-ethyl sinapate, photoexcited at 329 nm, the respective maxima in the UV/vis absorption spectra.

isomer photoproduct, we are unable to observe the presence of the isomer photoproduct in our TAS at 2ns.

The kinetics contained within the TAS were recovered using, a sequential ($A \xrightarrow{\tau_1} B \xrightarrow{\tau_2} C \xrightarrow{\tau_3} D \xrightarrow{\tau_4} E$) global fitting technique, using the software package Glotaran.⁷ The resulting time-constants (τ_n) are provided in Table S1. Furthermore, an additional time-constant is required to accurately fit the TAS of ethyl sinapate in ethanol compared to cyclohexane. We discuss this in more detail below. The evolution associated difference spectra (EADS) and fit residuals are shown in Figure S10 and 11 respectively.

Table S1: The resulting time-constants from the sequential global fit of the TAS. τ_{ivr} is the timescale for intramolecular vibrational rearrangement (IVR), τ_{iet} which is absent in cyclohexane, corresponds to the timescale for intermolecular energy transfer (IET), τ_{iso} represents the time-constant for the photoisomerization, while the time-constant τ_{pp} represents the lifetime of the photoproduct absorption. Note that τ_{pp} is significantly longer than our maximum experimentally achievable Δt (2 ns).

	τ_{ivr}	τ_{iet}	τ_{iso}	τ_{pp}
Z-ethyl sinapate	140 ± 40 fs	2.11 ± 0.04 ps	30.5 ± 0.5 ps	$>> 2$ ns
E-ethyl sinapate	120 ± 40 fs	2.38 ± 0.04 ps	30.8 ± 0.4 ps	$>> 2$ ns

The ultrafast dynamics of sinapates in a polar environment have been explored before and therefore we shall draw upon the literature in order to assign each time-constant.^{4,5,8}

Firstly, considering τ_{ivr} , this time-constant is a geometry rearrangement of the excited-state molecule away from the initially prepared Franck-Condon region (as in cyclohexane). However, we are unable to comment on the differences between the isomers regarding this time-constant as these are within our time-resolution/experimental error.

The second time-constant τ_{iet} represents the timescale in which vibrational cooling of the excited state to the surrounding solvent bath occurs. Unlike τ_{ivr} , τ_{iet} has different values between the two isomers with the Z-isomer having a shorter time scale. The vibrational cooling of the excited state is not observed in cyclohexane, likely due to it occurring on a similar timescale to the photoisomerization.

Finally, τ_{iso} reports on the timescale for photoisomerization, as it corresponds to the decay of the ESA and the SE (and accords with previously measured time-constants in polar solvents^{4,5,8}). However, unlike ethyl sinapate in cyclohexane, where a 10% difference is seen in the time-constant, no apparent difference is present in the data obtained in ethanol.

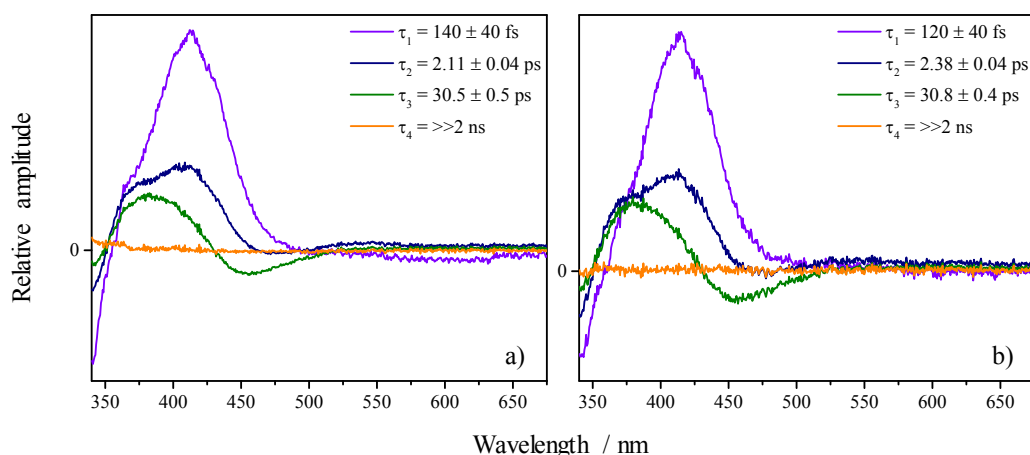


Figure S10: Resulting EADS from the sequential global fit of ethyl sinapate, a) Z-ethyl sinapate photoexcited at 327 nm and b) E-ethyl sinapate photoexcited at 329 nm in ethanol.

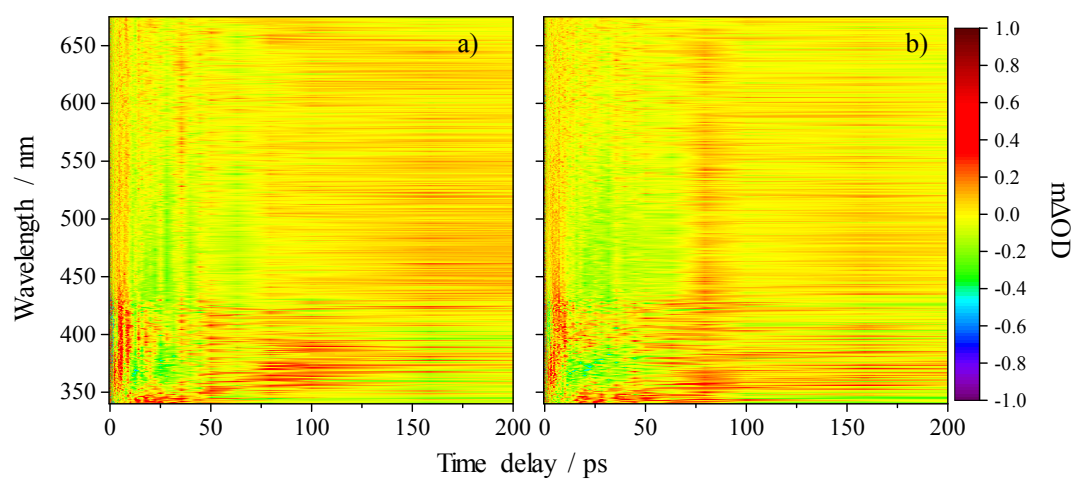


Figure S11: TAS residual plot with a maximum deviation of ~10% for a) Z-ethyl sinapate photoexcited at 327 nm and b) E-ethyl sinapate photoexcited at 329 nm in ethanol.

Refences

1. S. E. Greenough, M. D. Horbury, J. O. F. Thompson, G. M. Roberts, T. N. V. Karsili, B. Marchetti, D. Townsend and V. G. Stavros, *Phys. Chem. Chem. Phys.*, 2014, **16**, 16187-16195.
2. S. E. Greenough, G. M. Roberts, N. A. Smith, M. D. Horbury, R. G. McKinlay, J. M. Žurek, M. J. Paterson, P. J. Sadler and V. G. Stavros, *Phys. Chem. Chem. Phys.*, 2014, **16**, 19141-19155.
3. J. C. Dean, R. Kusaka, P. S. Walsh, F. Allais and T. S. Zwier, *J. Am. Chem. Soc.*, 2014, **136**, 14780-14795.
4. L. A. Baker, M. D. Horbury, S. E. Greenough, F. Allais, P. S. Walsh, S. Habershon and V. G. Stavros, *J. Phys. Chem. Lett.*, 2016, **7**, 56-61.
5. M. Horbury, W.-D. Quan, A. Flourat, F. Allais and V. Stavros, *Phys. Chem. Chem. Phys.*, 2017, **19**, 21127-21131.
6. M. Vengris, D. S. Larsen, M. A. van der Horst, O. F. A. Larsen, K. J. Hellingwerf and R. van Grondelle, *J. Phys. Chem. B*, 2005, **109**, 4197-4208.
7. J. J. Snellenburg, S. Liptonok, R. Seger, K. M. Mullen and I. H. M. Van Stokkum, *J. Stat. Softw.*, 2012, **49**.
8. J. Luo, Y. Liu, S. Yang, A. L. Flourat, F. Allais and K. Han, *J. Phys. Chem. Lett.*, 2017, **8**, 1025-1030.